CO_2 hydrogenation to methanol over $CuO–ZnO–TiO_2–ZrO_2$: a comparison of catalysts prepared by sol–gel, solid-state reaction and solution-combustion

Dawei Chen, Dongsen Mao, Jie Xiao, Xiaoming Guo & Jun Yu

Journal of Sol-Gel Science and Technology

ISSN 0928-0707
Volume 86
Number 3

J Sol-Gel Sci Technol (2018) 86:719-730
DOI 10.1007/s10971-018-4680-4

Springer

Journal of Sol-Gel Science and Technology (2018) 86:719–730
https://doi.org/10.1007/s10971-018-4680-4

ORIGINAL PAPER: SOL–GEL AND HYBRID MATERIALS FOR CATALYTIC, PHOTOELECTROCHEMICAL AND SENSOR APPLICATIONS

CO_2 hydrogenation to methanol over CuO–ZnO–TiO_2–ZrO_2: a comparison of catalysts prepared by sol–gel, solid-state reaction and solution-combustion

Dawei Chen[1] · Dongsen Mao[1] · Jie Xiao[1] · Xiaoming Guo[1] · Jun Yu[1]

Received: 27 February 2018 / Accepted: 7 May 2018 / Published online: 24 May 2018

Abstract

Three CuO–ZnO–TiO_2–ZrO_2 catalysts with the same composition were prepared through sol–gel, solid-state reaction, and solution-combustion methods and characterized by X-ray diffraction (XRD), N_2 adsorption, X-ray photoelectron spectroscopy (XPS), temperature-programmed reduction with H_2 (H_2-TPR), reactive N_2O adsorption, and adsorption of H_2 and CO_2 followed by temperature-programmed desorption (H_2-TPD, CO_2-TPD) techniques. Their catalytic performances for CO_2 hydrogenation to methanol were tested in a fixed-bed reactor under the conditions of 200–280 °C, 3 MPa, and SV = 2400 mL g_{cat}^{-1} h^{-1}. The results indicated that the texture, structure, reducibility, and adsorption capacity for reactants of the CuO–ZnO–TiO_2–ZrO_2 catalyst were affected noticeably by preparation methods and the catalyst prepared by sol–gel method exhibited the highest CO_2 conversion and methanol selectivity, which reached to 17.0% and 44.0%, respectively. The highest activity of the CuO–ZnO–TiO_2–ZrO_2 catalyst prepared by sol–gel method was attributed to the largest metallic Cu surface area and adsorption capacity for H_2.

Graphical Abstract

The catalyst prepared by sol–gel method exhibits the highest performance for methanol synthesis, which was attributed to the largest metallic Cu surface area and adsorption capacity for H_2.

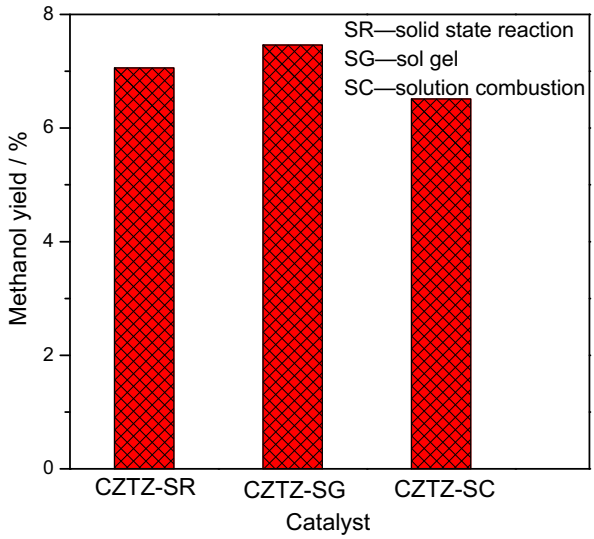

✉ Dongsen Mao
dsmao@sit.edu.cn

✉ Xiaoming Guo
guoxiaoming@sit.edu.cn

[1] School of Chemical and Environmental Engineering, Shanghai Institute of Technology, Shanghai 201418, China

Highlights

- $CuO–ZnO–TiO_2–ZrO_2$ catalyst was prepared by three different methods.
- The catalyst prepared by sol–gel method exhibited the highest yield of methanol.
- The catalyst prepared by solution combustion exhibited the lowest methanol yield.
- The superior activity of the sol–gel method derived catalyst was attributed to the largest S_{Cu}.

Keywords $CuO–ZnO–TiO_2–ZrO_2$ catalyst · sol–gel method · solid-state reaction method · solution-combustion method · CO_2 hydrogenation · methanol synthesis

1 Introduction

In recent years, the greenhouse effect resulted from CO_2 emissions becomes more and more serious. On the other hand, CO_2 is a valuable carbon resource in nature, which can be converted into useful chemicals and fuels [1, 2]. Accordingly, intensive research efforts have been recently focused on improving the efficiency for CO_2 hydrogenation to methanol because methanol is an important solvent and feedstock for the production of chemicals and fuel additives, which is of great significance for the sustainable development of society [3–5].

Nowadays, methanol is synthesized from syngas over a $CuO–ZnO–Al_2O_3$ catalyst. By the reason of low activity and stability of CO_2 hydrogenation over the $CuO–ZnO–Al_2O_3$ catalyst, searching for more efficient catalysts has attracted great interests [6–8]. Over the past years, it was found that the $CuO–ZnO–ZrO_2$ catalyst exhibited better performance for methanol synthesis from CO_2 hydrogenation [9–13]. Moreover, the addition of Ti was also found to promote the catalytic performance of Cu–ZnO-based catalysts for methanol synthesis from CO_2 hydrogenation [14–16]. The reason was that the promoters ZrO_2 and TiO_2 can enhance the dispersity of metallic copper and the adsorption capacity for CO_2 [14, 16, 17], and TiO_2 could also effectively inhibit the reverse water-gas shift reaction [18]. Therefore, the $CuO–ZnO–TiO_2–ZrO_2$ (CZTZ) catalyst had a considerably high activity for methanol synthesis from CO_2 hydrogenation [16].

On the other hand, the structure and the interaction among the components of a catalyst are greatly affected by its preparation methods, which in turn exerts an important influence on catalytic performance [12, 19–22]. Currently, the Cu-based catalysts for methanol synthesis are usually prepared by co-precipitation method [8, 12–17]. However, the procedure of the method was complex and time-consuming, which required precise pH control and long aging time of the suspension; furthermore, tedious washing was indispensable [23, 24]. Therefore, it was imperative and significant to develop novel and effective techniques for preparing the Cu-based catalysts. Recently, Guo et al. investigated the solution-combustion [10, 19] and solid-state reaction [20] methods for the preparation of $CuO–ZnO–ZrO_2$ catalyst, and the results showed that the high dispersion of Cu led to a larger interfacial area between Cu and other oxides, which was considered to be the key to obtain the high activity and selectivity [25, 26]. On the other hand, sol–gel method can gain a larger surface area and higher dispersity of the active species throughout the catalyst, so it has attracted considerable attention as a preparation method of catalysts [27, 28]. However, it has been rarely used in the preparation of Cu–ZnO-based catalyst for the synthesis of methanol [21].

In this work, CZTZ catalyst was prepared by citric acid sol–gel method, and compared with the counterparts prepared by solution-combustion and solid-state reaction methods using the citric acid as fuel and complex agent. The structural and textural properties of the prepared CZTZ catalysts were characterized by XRD, N_2 adsorption, XPS, H_2-TPR, reactive N_2O adsorption, H_2-TPD, and CO_2-TPD techniques. Their catalytic performances in methanol synthesis from CO_2 hydrogenation were then investigated and compared. Furthermore, the differences in catalytic performance of the CZTZ catalysts prepared by different methods were discussed profoundly in relation to the results of physicochemical characterizations.

2 Experimental

2.1 Catalyst preparation

Three CZTZ catalysts with the same composition were prepared by three different methods, i.e., sol–gel, solution-combustion and solid-state reaction, in which the proportion of Cu:Zn:Ti:Zr = 40:40:10:10 (atom ratio) was chosen on the basis of our previous study [16]. The molar ratio of the citric acid to the total metal ions was 1.2:1 to ensure all the metal ions to be completely reacted. All chemicals were of analytical grade and used as received (Shanghai Chemical Reagent Corporation, China) without further purification.

Sol–gel method (SG): The required amounts of $Cu(NO_3)_2{\cdot}3H_2O$, $Zn(NO_3)_2{\cdot}6H_2O$, and $Zr(NO_3)_4{\cdot}5H_2O$ were dissolved into 20 mL ethanol, and mixed with the required amount of tetrabutyl titanate (TBT). Subsequently, a citric acid solution (dissolved in 30 mL of ethanol) was added to

the above mixed solution with constant stirring at 70 °C. After the mixed liquor became a sol, the sol was dried in an oven at 110 °C for 12 h and transformed into a gel. Finally, the dried gel was calcined at 400 °C (heating rate of 5 °C/min) for 4 h in a muffle furnace.

Solid-state reaction method (SR): First, the required amounts of nitrates of Cu, Zn, Zr, and TiO_2 were blended in solid state to form a premix; then the citric acid was added to the premix and ground in an agate mortar. After half an hour, the precursor was dried in an oven at 110 °C for 12 h. Finally, the dried sample was ground in a crucible and was calcined at 400 °C (heating rate of 5 °C/min) for 4 h in a muffle furnace.

Solution-combustion method (SC): The required amounts of nitrates of Cu, Zn, and Zr were dissolved into an appropriate amount of ethanol, and mixed with the required amount of TBT. Then a citric acid solution (dissolved in 30 mL of ethanol) was added to the mixed solution with constant stirring. The resulting mixture was sonicated to get a clear blue solution. The solution was transferred to a muffle furnace which was preheated to 350 °C. With the evaporation of ethanol, the solution was transformed into a viscous gel and then the blistering combustion occurred. Meanwhile, large amounts of gas released and the combustion ended up in a few minutes. Afterwards, the sample was further calcined at 400 °C (heating rate of 5 °C/min) for 4 h.

These CZTZ catalysts prepared by sol–gel, solid-state reaction, and solution combustion methods were denoted as CZTZ-SG, CZTZ-SR, and CZTZ-SC, respectively.

2.2 Catalyst characterization

XRD patterns were recorded with a PANalytical X'Pert diffractometer operating with Ni β-filtered Cu K-α radiation at 40 kV and 40 mA. The 2θ range was scanned from 10° to 80° by steps of 6° in 1 min.

N_2 adsorption and desorption isotherms of the catalysts were measured by a Micromeritics ASAP2020 M + C adsorption apparatus. Full nitrogen adsorption/desorption isotherms at −196 °C were obtained after outgassing the sample under vacuum at 200 °C for 10 h. The specific-surface area and pore volume were calculated by BET and BJH models, respectively.

The exposed Cu surface area (S_{Cu}) was obtained by dissociative N_2O adsorption, using a Ramiin GC 2060 instrument through the procedure described in the literature [22]. Briefly, the catalyst (0.1 g) was first placed in a fixed-bed reactor and reduced in a 10% H_2/N_2 mixture (30 mL/min) for 1 h at 300 °C. Afterwards, the reduced sample was cooled to 60 °C and isothermally purged with N_2 for 30 min; then the sample was flushed with N_2O (30 mL/min) for 1 h to ensure complete oxidation of surface metallic copper. Next, the sample was ventilated with N_2 to remove the N_2O for 30 min and cooled to room temperature (25 °C). Finally, a 10% H_2/N_2 mixture (30 mL/min) was contact with the catalyst and the temperature was raised to 300 °C at a rate of 2 °C/min. The surface copper ions were reduced and the S_{Cu} of the catalyst was calculated by the following equation [29]:

$$S_{Cu} = (2n_{H_2} \times N)/\left(1.46 \times 10^{19} \times W\right) \quad (1)$$

in which, S_{Cu} was the exposed copper surface area per gram catalyst, n_{H_2} was molar number of consumed H_2 after reoxidation of the catalyst surface by N_2O, N was Avogadro constant (6.02×10^{23} atoms/mol), 1.46×10^{19} was the number of copper atoms per square meter, and W was the weight of the catalyst.

H_2-TPR experiments were performed in a continuous-flow apparatus fed with a 10% H_2/N_2 mixture flowing at 50 mL/min and heated to 300 °C at a speed of 10 °C/min. A quantity of 30 mg of catalyst was used, and H_2 consumption was monitored by a thermal conductivity detector (TCD).

H_2-TPD was performed in a quartz tubular reactor. First, the catalyst was reduced at 300 °C for 1 h in a flowing of 10% H_2/N_2 mixture. Then, the sample was cooled to room temperature (25 °C) and further saturated in H_2/N_2 mixture for 30 min; then flushed by N_2 stream until stabilization of the baseline of the TCD signal. The TPD measurements were carried out in a N_2 stream (30 mL/min) from 50 °C to 500 °C at a heating rate of 5 °C/min. The process of desorption was monitored by a TCD.

The basicity of the catalyst was measured by CO_2-TPD. First, the catalysts were reduced at 300 °C for 1 h in a flow of 10% H_2/N_2 mixture. Then the reduced catalysts were cooled to 50 °C and further saturated in 10% CO_2/N_2 mixture (30 mL/min) for 30 min. Subsequently, a flow of He passed over the catalysts for 1 h to remove any physisorbed molecules. Afterwards, the TPD experiment was started at a heating rate of 5 °C/min from 50 to 450 °C under He flow (30 mL/min), and the CO_2 desorption processes was monitored by a mass spectrometer (Pefeiffer Vacuum Quadstar, 32-bit).

XPS measurements were performed using a Thermo Scientific ESCALAB 250Xi spectrometer equipped with an Al Kα X-ray exciting source (1486.6 eV) from the Surface Science Instruments. The samples were pressed into small double side tap on a multi-specimen stage. Before recording spectra, the samples were outgassed overnight under $p < 10^{-8}$ kPa in the preparation chamber and introduced into the analysis chamber where the pressure was around 10^{-7} kPa. The pass energy of the analyzer was set at 150 eV, and the spot size was ~1.4 mm^2. Besides, all binding energies were calculated according to the standardizing C 1 s peak at 284.6 eV (accuracy within ±0.3 eV). Peak decomposition

was performed using the Casa XPS program (Casa Software Ltd, UK) with a Gaussian/Lorentzi (85/15) product function and a Shirley nonlinear sigmoid-type baseline. The following peaks were used for the quantitative analysis: O 1s, C 1s, Cu $2p_{3/2}$, Zn $2p_{3/2}$, Ti $2p_{3/2}$, and Zr $3d_{5/2}$.

2.3 Catalytic activity testing

The evaluation of catalytic performance in CO_2 hydrogenation was carried out in a continuous flow, fixed-bed reactor operating at 200–280 °C and 3.0 MPa. A CO_2–H_2–N_2 gas mixture in the molar ratio of 22:66:12 was fed with a speed of 20 mL/min over 0.5 g catalysts (40–60 mesh) diluted with 0.5 g same-sized quartz sand packed into the stainless steel tubular reactor (5 mm i.d.). Prior to the catalytic measurements, the catalysts were reduced at 300 °C for 3 h in a stream of 10% H_2/N_2 (30 mL/min) under atmospheric pressure. All lines and valves of reaction equipment were heated to 170 °C by heating band to prevent product condensation. Effluent reaction stream was analyzed on-line with a gas chromatograph (6820, Agilent) equipped with a two-column system, which is connect to a flame-ionization detector (FID) (for CH_3OH) and a TCD (for CO, N_2, CO_2), respectively. Conversion of CO_2 (X_{CO_2}), selectivity of CO and methanol (S_{CO}, S_{CH_3OH}), and yield of methanol (Y_{CH_3OH}) were calculated according to Eqs. (2)–(5) and the steady-state values were quoted as the average of three different analyses taken after 4 h on stream operation.

$$X_{CO_2}\% = \frac{A_{CO}\cdot f_{CO} + A_{CH_3OH}\cdot f_{CH_3OH}}{A_{CO}\cdot f_{CO} + A_{CH_3OH}\cdot f_{CH_3OH} + A_{CO_2}\cdot f_{CO_2}} \times 100 \quad (2)$$

$$S_{CO}\% = \frac{A_{CO}\cdot f_{CO}}{A_{CO}\cdot f_{CO} + A_{CH_3OH}\cdot f_{CH_3OH}} \times 100 \quad (3)$$

$$S_{CH_3OH}\% = \frac{A_{CH_3OH}\cdot f_{CH_3OH}}{A_{CO}\cdot f_{CO} + A_{CH_3OH}\cdot f_{CH_3OH}} \times 100 \quad (4)$$

$$Y_{CH_3OH}\% = X_{CO_2}\% \times S_{CH_3OH}\% \quad (5)$$

where, A_i represented the integral peak areas of products (CO and methanol) or reactant CO_2 in the GC analysis, and f_i represented their correction factors.

Turn over frequency for methanol synthesis (TOF_{MeOH}), which represents the molecular number of methanol formed per second per metallic copper atom, was calculated by the following equation [30]:

$$TOF_{MeOH}\left(S^{-1}\right) = \frac{A \cdot N_a}{3600 \cdot S_{Cu} \cdot N_a} \quad (6)$$

where, A is the methanol activity (mol h^{-1} g^{-1}); N_a is the Avogadro constant (6.02×10^{23}); S_{Cu} is the metallic copper surface area (m^2/g); N_a is the number of Cu atoms in a monolayer (1.46×10^{19} atoms/m^2).

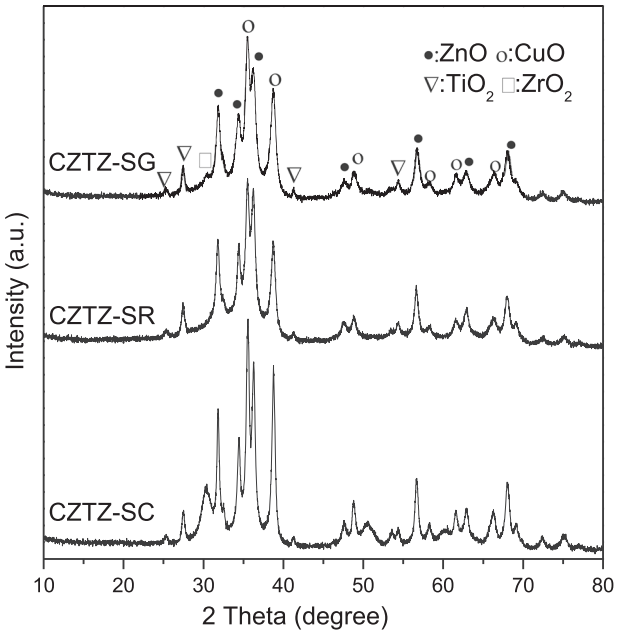

Fig. 1 XRD patterns for different CuO–ZnO–TiO_2–ZrO_2 catalysts

3 Results and discussion

3.1 Characterization of the calcined samples

3.1.1 XRD analysis

Figure 1 shows the XRD patterns of the CZTZ catalysts prepared by different methods and calcined at 400 °C. The diffraction peaks at 35.5°, 38.7°, 48.7°, 53.7°, 58.3°, 61.6°, and 66.3° can be attributed to the presence of CuO phase (PDF#48-1548), while the diffraction peaks at 31.8°, 34.3°, 36.2°, 47.8°, 56.7°, 62.9°, and 68.0° are indicative of the presence of ZnO phase (PDF#36-1451). The only diffraction peak of ZrO_2 locates at 30.3°, and several diffraction peaks of TiO_2 are found at 25.2°, 27.4°, 41.3°, and 54.4° [31]. As shown in Fig. 1, the diffraction peak of ZrO_2 cannot be observed on the CZTZ-SR sample, suggesting that the ZrO_2 is amorphous or high-dispersed on the catalyst surface [32]. For the diffraction peaks of TiO_2, no noticeable differences in intensity and broadness can be observed among all catalysts, indicating that the different preparation methods have no effect on the crystallinity of TiO_2. On the other hand, the diffraction peaks of CuO and ZnO in the CZTZ-SC sample are stronger and narrower than those of the other two catalysts, indicating that the CZTZ-SC sample possesses a better crystallinity and larger sizes of CuO and ZnO particles. The mean sizes of CuO and ZnO crystallites over different catalysts were estimated using the Scherrer

Table 1 Physicochemical properties of different catalysts

Catalyst	S_{BET} (m^2/g)	Pore volume (cm^3/g)	Pore diameter (nm)	D^a_{CuO} (nm)	D^a_{ZnO} (nm)	D^a_{Cu} (nm)	S^b_{Cu} (m^2/g)	$TOF_{CH3OH} \times 10^3$ (S^{-1})
CZTZ-SG	43.1	0.12	11.5	15.2	15.3	16.4	2.25	8.3
CZTZ-SR	38.2	0.12	12.3	15.9	20.2	18.8	2.10	8.4
CZTZ-SC	31.7	0.14	17.4	19.5	22.3	19.6	1.88	8.6

[a]Determined by Scherrer equation

[b]Determined by N_2O chemisorption method

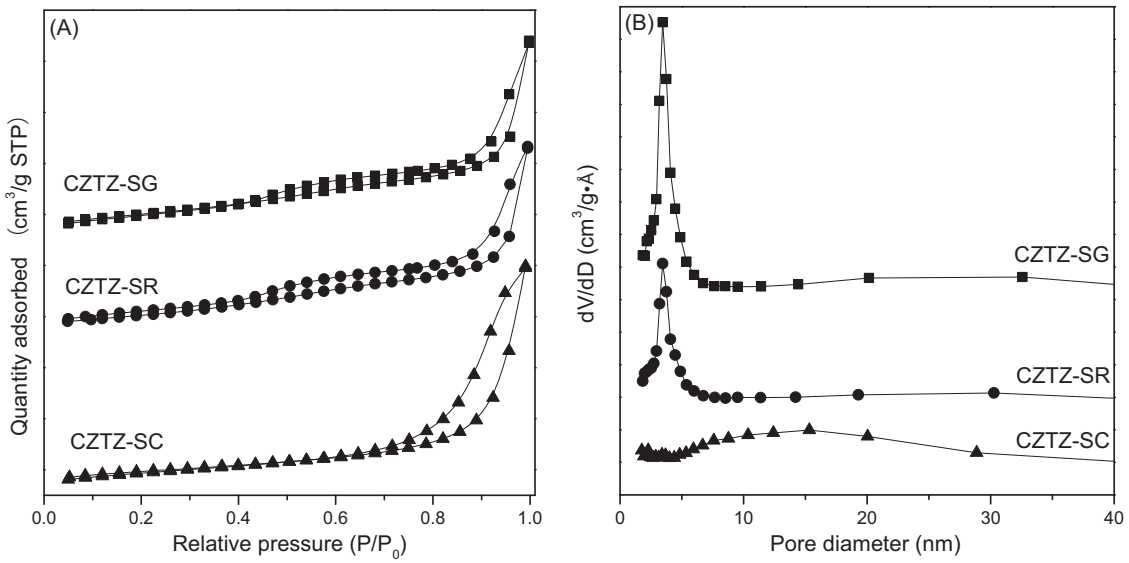

Fig. 2 N_2 adsorption-desorption isotherms (A) and the corresponding pore size distribution curves (B) of different catalysts

equation and both of them increased in the order of CZTZ-SG < CZTZ-SR < CZTZ-SC (Table 1).

3.1.2 N_2 adsorption study

N_2 adsorption-desorption isotherms and the corresponding pore size distribution curves of the different catalysts are presented in Fig. 2. As seen from Fig. 2a, all the samples exhibit type IV isotherms with H3-type hysteresis loops according to the classification of the adsorption isotherm, indicating that all the catalysts are mesoporous material. Moreover, the hysteresis loop of CZTZ-SC is larger than those of the other two catalysts, indicating that it owns a bigger mesopore volume. The reason is probably that the CZTZ-SC sample was prepared from the fast combustion of a solution containing citric acid. Therefore, it generated a lot of heat and gas due to the burning of the large amount of citric acid, leading to larger grains, pore volume, and pore diameter. Nevertheless, the other two samples experienced a drying process before the calcination, thus the free citric acid evaporated so that the resulted grains, pore volume, and pore diameter are smaller. From Fig. 2b, the samples of CZTZ-SG and CZTZ-SR exhibit one centralized pore distribution at 4.2 nm, but CZTZ-SC has a very broad pore distribution with a maximum at 16.1 nm. This result indicates that the catalyst prepared by solution-combustion has a significantly wider pore distribution than the other two catalysts. The main textural parameters of the samples are collected in Table 1. As seen, the S_{BET} decreases in the order of CZTZ-SG > CZTZ-SR > CZTZ-SC; while the pore diameter increases in the order of CZTZ-SG < CZTZ-SR < CZTZ-SC. These results are in agreement with the crystallite sizes of CuO and ZnO as shown in Table 1. On the other hand, no distinct disparity between the pore volumes can be observed among these catalysts.

3.1.3 XPS analysis

The surface chemical properties of the CZTZ catalysts were investigated by XPS. The patterns of the Cu 2p, Zn 2p, Ti 2p, and Zr 3d for the catalysts are shown in Fig. 3 and the corresponding binding energies (BE) of Cu $2p_{3/2}$, Zn $2p_{3/2}$, Ti $2p_{3/2}$, and Zr $3d_{5/2}$ core electrons are summarized in Table 2. As shown in Fig. 3a, the Cu $2p_{3/2}$ and Cu $2p_{1/2}$ peaks appeared at around 933 and 953 eV, accompanied by a shake-up peak at 938–945 eV for all the catalysts,

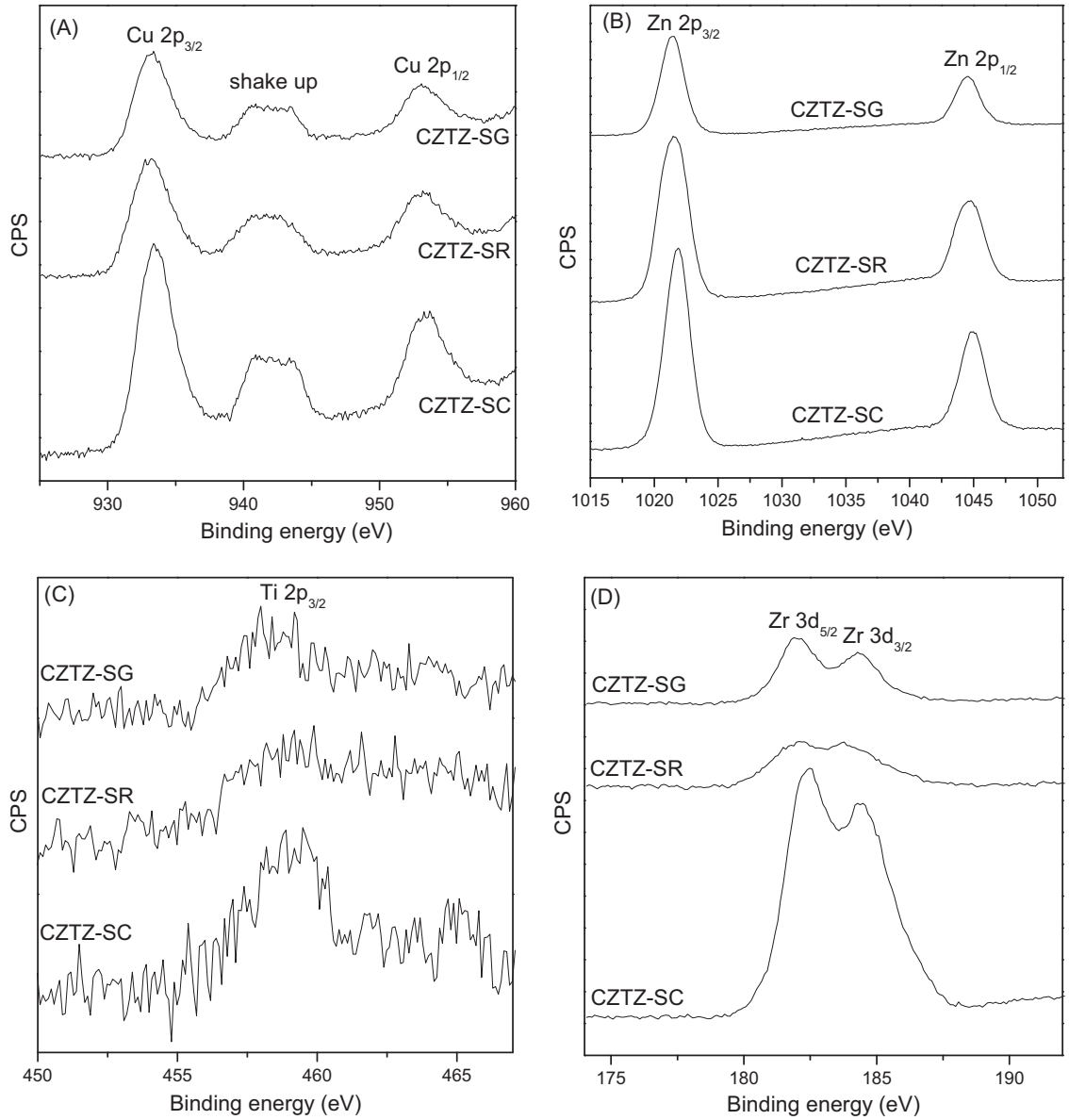

Fig. 3 XPS patterns for different catalysts: **a** Cu, **b** Zn, **c** Ti, and **d** Zr

revealing that the chemical state of copper in all the calcined samples was +2 [14, 16]. For Zn $2p_{3/2}$ electrons, its position (Fig. 3b) at about 1022 eV was characteristic of ZnO species [14, 16]. The BE of Ti $2p_{3/2}$ was at 458–459 eV, which is in good agreement with the reported values for Ti^{4+} [14, 16]. The BE of Zr $3d_{5/2}$ was at 182 eV, which suggests that zirconium species is in the form of ZrO_2 [16]. These results suggest that the chemical states of Cu, Zn, Ti, and Zr on the different CZTZ catalyst are identical.

Table 2 lists the metal contents on the surface of the CZTZ samples measured by the XPS technique. The results indicate that the surface of all the samples is "zinc-rich, copper-depleted". Similar results were also reported by some researchers on other CuO–ZnO-based catalysts [16, 20, 33]. In addition, the Ti content on the surface of the three samples is remarkably lower than the nominal value (10 at.%). Whereas, the Zr content on the surface of CZTZ-SC is significantly higher than the nominal one (10 at.%), indicating that excessive ZrO_2 cover a part of CuO. Meanwhile, the relative surface concentration of Zn in CZTZ-SR is much higher than the nominal one (40 at.%), suggesting that the surface of CuO is covered partly by an excess of ZnO on the CZTZ-SR catalyst.

3.1.4 H_2-TPR determination

To assess the reduction behavior of the catalysts, TPR measurements of the different CZTZ catalysts were carried

Table 2 XPS results of different CuO–ZnO–TiO_2–ZrO_2 catalysts

Catalyst	Binding energy (eV)				Relative surface concentration of metal (at.%)			
	Cu $2p_{3/2}$	Zn $2p_{3/2}$	Ti $2p_{3/2}$	Zr $3d_{5/2}$	Cu	Zn	Ti	Zr
CZTZ-SG	933.5	1021.4	458.0	182.2	29.1	57.0	2.5	11.4
CZTZ-SR	933.3	1021.5	458.3	182.9	22.5	68.9	1.6	7.0
CZTZ-SC	933.4	1021.8	459.0	182.9	23.2	52.3	2.8	21.7

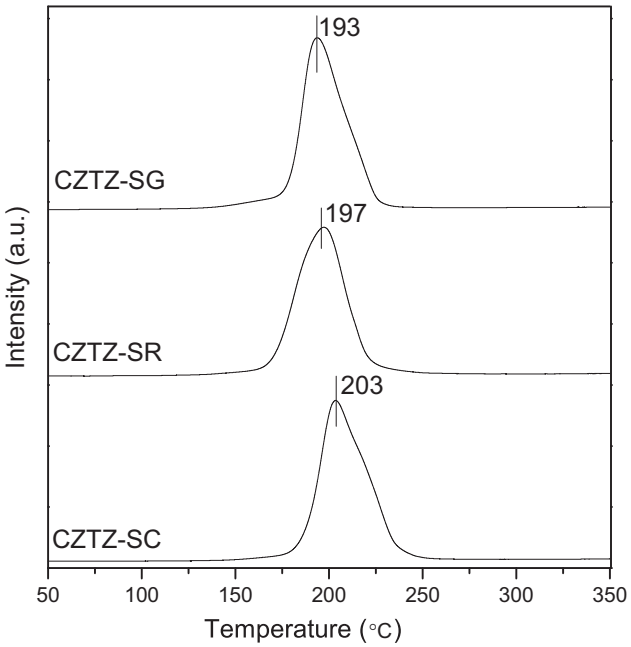

Fig. 4 H_2-TPR patterns of different CuO–ZnO–TiO_2–ZrO_2 catalysts

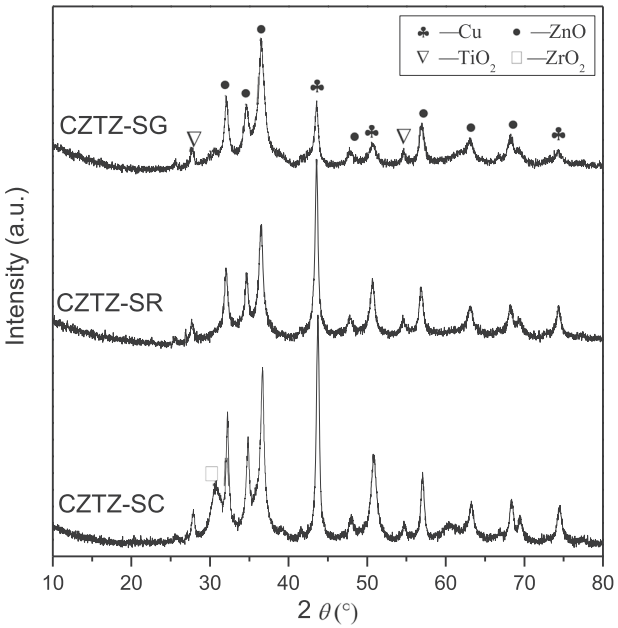

Fig. 5 XRD patterns of different catalysts after reduction at 300 °C

out and the results are shown in Fig. 4. It can be noted that all the TPR curves appear only one reduction peak in the temperature range of 160–250 °C. Since ZnO, ZrO_2, and TiO_2 cannot be reduced under the temperature below 300 °C, the reduction peak can be attributed to the reduction of CuO species [16]. Moreover, the temperature of reduction peak increases in the order of CZTZ-SG < CZTZ-SR < CZTZ-SC, indicating that the size of CuO particles increases from CZTZ-SG to CZTZ-SC because the smaller the CuO particle is, the lower the reduction temperature will be [20]. This result is in good line with the sizes of CuO crystallites determined by XRD analysis (Table 1).

3.2 Characterization of the reduced catalysts

3.2.1 XRD analysis

Figure 5 shows the XRD patterns of the different catalysts after in situ reduction in H_2 at 300 °C. It can be seen that all the catalysts exhibit three diffraction peaks at 43.5°, 50.7°, and 74.4°, which are respectively characteristic of Cu(111), Cu(200), and Cu(220) planes. There are no diffraction peaks of CuO detectable for all samples, indicating that the CuO are totally reduced to metallic copper. As seen in Table 1, the variation trend of crystallite size of metallic copper is the same as that of CuO in the calcined catalysts. On the other hand, no noticeable changes in positions and intensity of the diffraction peaks corresponding to ZnO, TiO_2, and ZrO_2 can be observed, suggesting that these oxides were not reduced under the present reduction conditions.

3.2.2 XPS investigation

The XPS spectra of the CZTZ catalysts after in situ reduction at 300 °C are shown in Fig. 6. The BE values of Cu $2p_{3/2}$, Zn $2p_{3/2}$, Ti $2p_{3/2}$, and Zr $3d_{5/2}$ core electrons are summarized in Table 3. As shown in Fig. 6a, after reduction, the shake-up feature disappeared and the BE values of Cu $2p_{3/2}$ and Cu $2p_{1/2}$, respectively, decreased to 932.1 and 952.1 eV, indicating that the CuO species in the calcined samples has been reduced to metallic copper [34]. In contrast, the BE values of Zn $2p_{3/2}$, Ti $2p_{3/2}$, and Zr $3d_{5/2}$ in the CZTZ catalysts after reduction experienced no variations compared with the calcined catalysts, suggesting that the other components except CuO in the catalysts cannot be

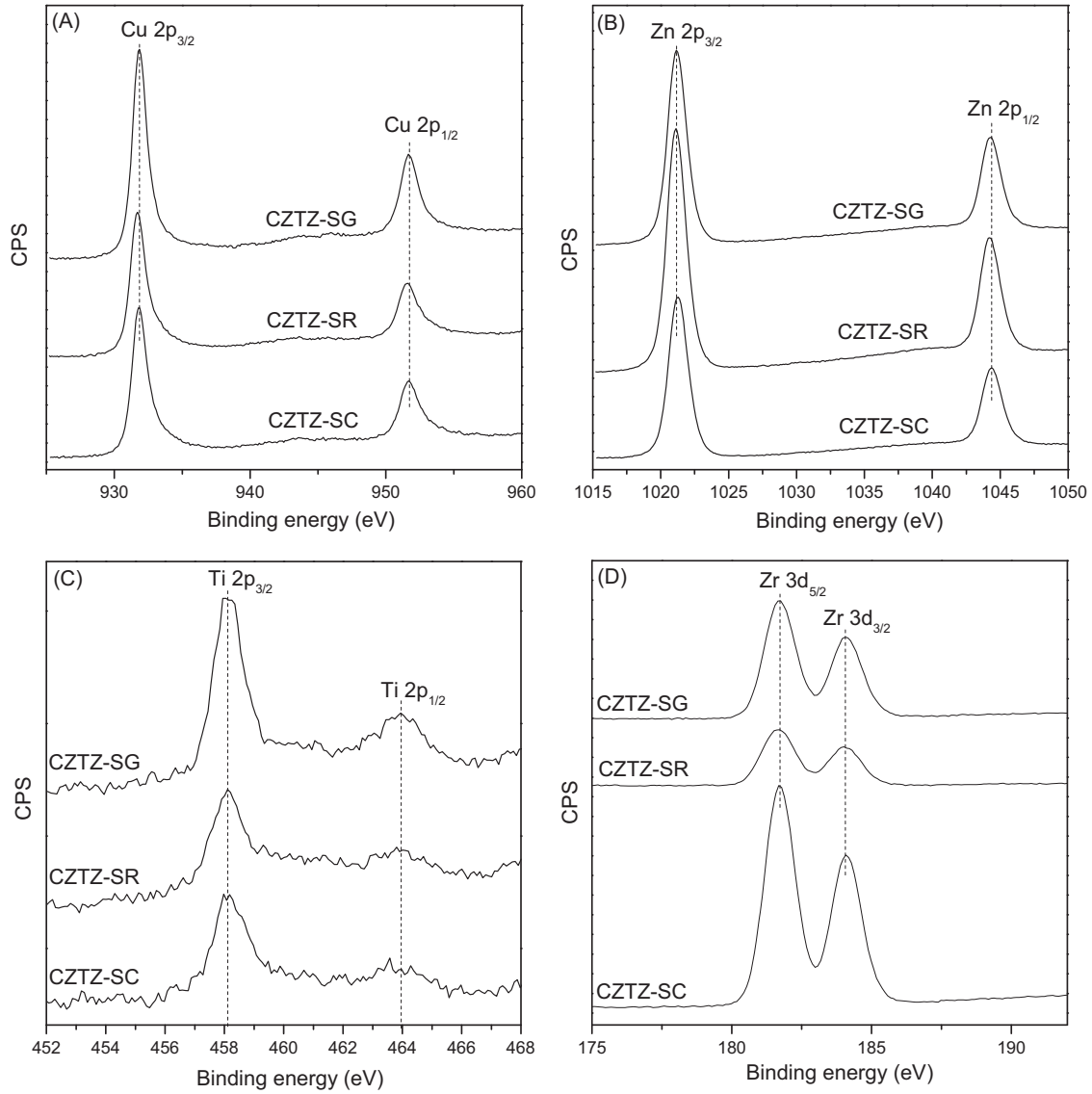

Fig. 6 XPS patterns of different catalysts after reduction: **a** Cu, **b** Zn, **c** Ti, and **d** Zr

Table 3 XPS results of different catalysts after reduction

Catalyst	Binding energy (eV)				Relative surface concentration of metal (at.%)			
	Cu $2p_{3/2}$	Zn $2p_{3/2}$	Ti $2p_{3/2}$	Zr $3d_{5/2}$	Cu	Zn	Ti	Zr
CZTZ-SG	932.1	1021.2	458.3	182.6	22.9	59.8	3.1	14.2
CZTZ-SR	932.1	1021.3	458.3	182.6	16.7	74.1	2.1	7.1
CZTZ-SC	932.2	1021.3	458.3	182.6	21.1	51.5	2.1	25.3

reduced. These results are in line with those obtained by the above XRD measurements (Fig. 5).

Table 3 lists the metal content of the CZTZ samples after in situ reduction at 300 °C on the catalyst surface measured by the XPS measurements. The results indicate that the surface of samples is also "zinc-rich, copper-depleted" [35, 36]. Moreover, by combining the data in Table 2 and 3, it can be concluded that the "zinc-rich, copper-depleted" phenomenon was more severe after reduction, which is in agreement with the literature [37].

3.2.3 S_{Cu} measurement

The S_{Cu} values of the reduced CZTZ catalysts prepared by different methods are presented in Table 1. As seen, the S_{Cu} decreases in the order of CZTZ-SG > CZTZ-SR > CZTZ-

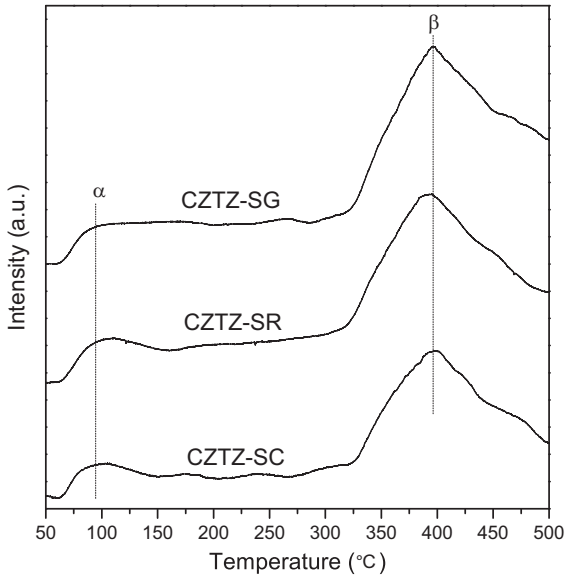

Fig. 7 H_2-TPD patterns of different catalysts after reduction

SC. Since the value of S_{Cu} is a mirror of the dispersion of Cu [10], it can be inferred that the CZTZ-SG and CZTZ-SC samples possess the highest and the lowest dispersion of Cu, respectively. This result is in good agreement with the size of Cu particles as determined by the XRD technique (Table 1).

3.2.4 H_2-TPD analysis

The H_2-TPD profiles for the different CZTZ catalysts are presented in Fig. 7, and the quantitative data of H_2 desorbed from the catalysts are summarized in Table 4. As seen in Fig. 7, the profile of all catalysts exhibits two desorption peaks in a wide temperature range (60–500 °C), which are denoted as peak α (at low temperature) and peak β (at high temperature), respectively. The two desorption peaks represent different hydrogen species adsorbed on the catalyst surface. According to literature [14, 16, 38], the α peak centered at about 95 °C was ascribable to the desorption of atomic hydrogen from metallic Cu on the catalyst surface; while the β peak centered at about 395 °C was due to the desorption of strongly adsorbed hydrogen from either the bulk of Cu particles or ZnO surface. From Fig. 7 it can be seen that the temperatures at maximum (T_{max}) of both α and β peaks for all the catalysts remain basically unchanged, indicating that the hydrogen adsorption strength of all the catalysts is almost the same. However, the amount of hydrogen desorbed from surface copper active sites (a peak) decreases in the order of CZTZ-SG > CZTZ-SR > CZTZ-SC. This is in accordance with the order of S_{Cu}. It should be emphasized that the reaction temperature in the present activity measurement was below 300 °C, so the hydrogen species desorbed at low-temperature is more conducive to the synthesis of methanol from CO_2 hydrogenation [14, 16].

Table 4 The amounts of H_2 and CO_2 desorbed from different catalysts

Catalyst	Amount of H_2 desorbed		Amount of CO_2 desorbed	
	A_α (a.u.)	A_β (a.u.)	A_α (a.u.)	A_β (a.u.)
CZTZ-SG	83	427	253	111
CZTZ-SR	72	409	412	137
CZTZ-SC	70	353	200	138

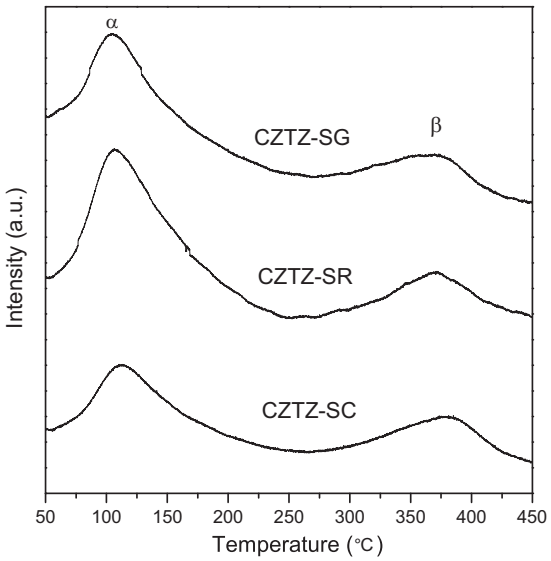

Fig. 8 CO_2-TPD patterns of different catalysts after reduction

3.2.5 CO_2-TPD study

Figure 8 depicts the CO_2-TPD patterns of the reduced CZTZ catalysts prepared by different methods. As seen, two broad desorption peaks could be observed over all the catalysts. The first one (denoted as peak α) at low temperature (60–210 °C) is ascribable to the weak basic site, while the second one in the range of 300–440 °C (denoted as peak β) represents the strong basic site. It was worth noting that the T_{max} of both α and β peaks in all the catalysts were almost the same, indicating that the strength of basic sites on the CZTZ catalyst was not affected noticeably by the different preparation methods. The quantitative data of CO_2 desorbed from different catalysts are also listed in Table 4. It can be seen that the amount of weak basic site decreases in the following order: CZTZ-SR > CZTZ-SG > CZTZ-SC. However, the amount of strong basic sites on different catalysts is similar. Considering that the actual reaction temperature in the present study was in the range of 200–280 °C, the desorption of CO_2 from low temperature seems to be rather

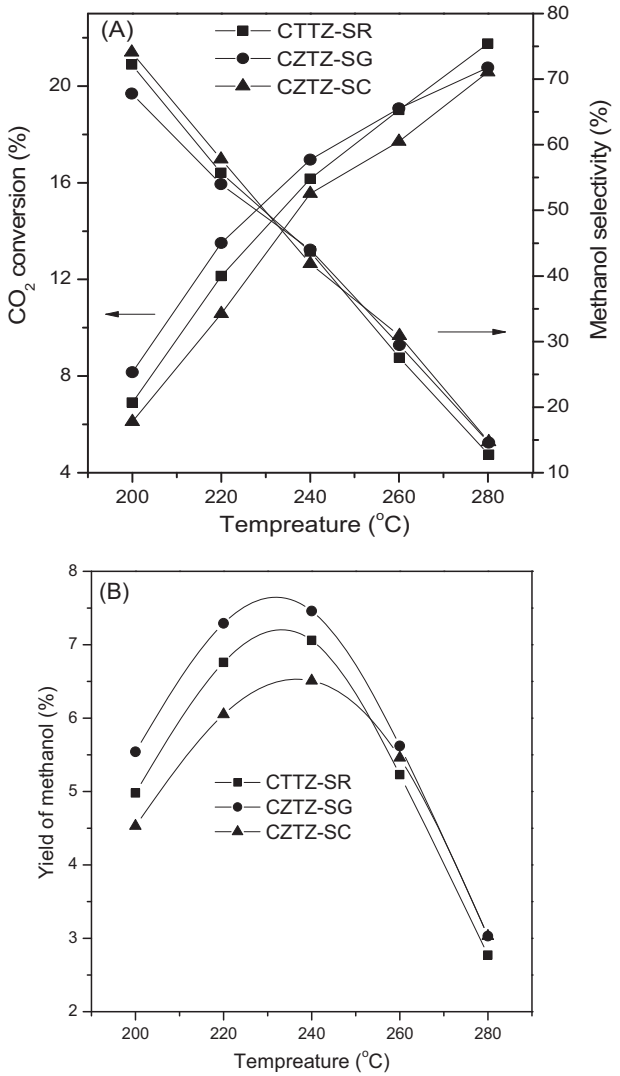

Fig. 9 Effect of reaction temperature on catalytic performance of different catalysts. **a** CO_2 conversion and methanol selectivity, **b** yield of methanol. Reaction conditions: $H_2/CO_2 = 3$ (v/v), P = 3.0 MPa, SV = 2400 mL g_{cat}^{-1} h^{-1}

associated with the active site for the CO_2 hydrogenation than that from high temperature [14, 39].

3.3 Catalytic performance

The results of the effect of reaction temperature on the catalytic performance of all the catalysts are presented in Fig. 9. In the present reaction conditions, methanol and CO were the only carbon-containing products. As shown in Fig. 9a, the conversion of CO_2 increased while the methanol selectivity decreased gradually with the increase of reaction temperature. Since the CO_2 hydrogenation to methanol reaction is exothermic, a low-temperature favors the synthesis of methanol. The changes of methanol yield with reaction temperature are presented in Fig. 9b; it is clear that there exists a maximum methanol yield which represents the

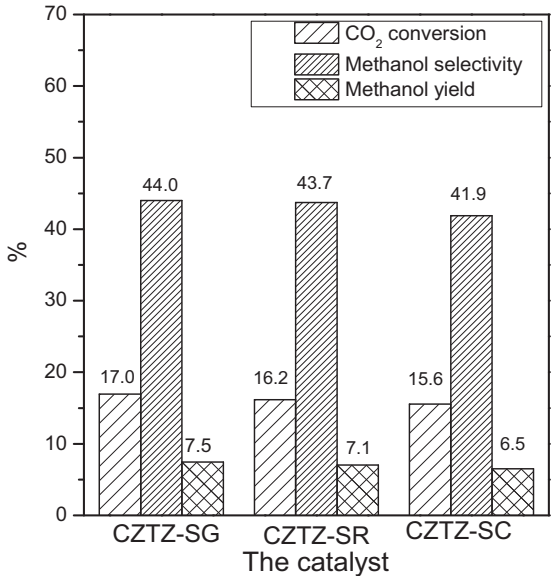

Fig. 10 Effect of preparation methods on catalytic performance of CZTZ catalysts. Reaction condition: $T = 240$ °C, $H_2/CO_2 = 3$(v/v), $P = 3.0$ MPa, SV = 2400 mL h^{-1} g_{cat}^{-1}

critical point of the reaction transforming from kinetics to thermodynamics [10]. Furthermore, the difference in the methanol yield between the different catalysts at low-reaction temperatures (≤240 °C) is significantly larger than that at high-reaction temperatures (≥260 °C) due to the thermodynamic limitation [39].

Activity and selectivity results for methanol synthesis from CO_2 hydrogenation over the different CZTZ catalysts at 240 °C are summarized in Fig. 10. As seen, both CO_2 conversion and methanol selectivity decrease in the order of CZTZ-SG > CZTZ-SR > CZTZ-SC.

It is well known that there are many factors that can affect the activity of the Cu-based catalysts for methanol synthesis from CO_2 hydrogenation. Based on the above characterization results, the causes of the difference between the catalytic activities of the CZTZ catalysts prepared by different methods can be attributed to the following: (1) different S_{Cu}. The results of XRD and S_{Cu} measurements show that the CZTZ catalysts prepared by different methods exhibit different sizes of Cu crystallites. As well known, different sizes of Cu crystallites may affect the yield of methanol through influencing the S_{Cu} and the TOF for methanol synthesis [9, 40, 41]. In this case, the relationship between the S_{Cu} and the yield of methanol are shown in Fig. 11 and it presents a perfect linear relationship. However, as shown in Table 1, the TOF for methanol formation remains basically constant regardless of the Cu particle sizes, which is in line with the result reported by Karelovic and Ruiz recently [42]. These results clearly indicate that the difference in the catalytic activity of the CZTZ catalysts prepared by different methods can be well

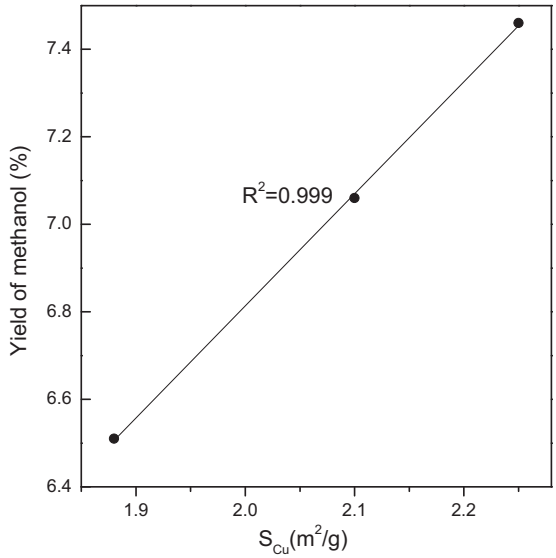

Fig. 11 The relationships between S_{Cu} and the yield of methanol

ascribed to their different S_{Cu} but not TOF. In other words, the preparation methods affect the dispersion of Cu particles without changing the intrinsic activity of the CZTZ catalyst. (2) different adsorption capacity for H_2. Recently, a dual-site mechanism of CO_2 hydrogenation to methanol has been well accepted for the Cu-based catalysts [43–46]. According to this mechanism, the adsorption capacity for CO_2 and H_2 has an important influence on the activity for methanol synthesis [16, 30, 47–49]. In this work, the variation of CO_2 conversion (Fig. 10) is not consistent with the trend of the amount of CO_2 desorbed from low temperature (Fig. 8 and Table 4), but in line with that of H_2 desorbed from low temperature (Fig. 7 and Table 4). These results suggest that the difference in the catalytic activity of the CZTZ catalysts prepared by different methods can also be attributed to their different adsorption capacity for H_2 [47, 50].

4 Conclusions

In this work, the synthesis of methanol from CO_2 hydrogenation was performed over CuO–ZnO–TiO_2–ZrO_2 catalysts prepared through three different methods (sol–gel, solid-state reaction, and solution combustion methods). The results show that the performance of the catalysts for methanol synthesis was influenced by preparation methods; and the catalyst prepared by sol–gel method owned the highest yield of methanol while that prepared by solution combustion method exhibited the lowest methanol yield. The difference in the catalytic activity of the CZTZ catalysts prepared by different methods can be attributed to their different metallic Cu surface areas and adsorption capacity for H_2.

Acknowledgements Financial supports from the Shanghai Municipal Education Commission (13YZ117) and Science and Technology Commission of Shanghai Municipality (13ZR1441200) are gratefully acknowledged.

Compliance with ethical standards

Conflict of interest The authors declare that they have no conflict of interest.

References

1. Lim X (2015) How to make the most of carbon dioxide. Nature 526:628–630
2. Barbato L,Centi G,Iaquaniello G,Mangiapane A,Perathoner S, (2014) Trading Renewable Energy by using CO_2: An effective option to mitigate climate change and increase the use of renewable energy sources. Energy Technol 2:453–461
3. Olah GA, Prakash GKS, Goeppert A (2011) Anthropogenic chemical carbon cycle for a sustainable future. J Am Chem Soc 133:12881–12898
4. Jadhav SG, Vaidya PD, Bhanage BM, Joshi JB (2014) Catalytic carbon dioxide hydrogenation to methanol: a review of recent studies. Chem Eng Res Des 92:2557–2567
5. Arab S, Commenge J, Portha J, Falk L (2014) Methanol synthesis from CO_2 and H_2 in multi–tubular fixed–bed reactor and multi–tubular reactor filled with monoliths. Chem Eng Res Des 92:2598–2608
6. Studt F, Sharafutdinov I, Abild-Pedersen F, Elkjær CF, Hummelshøj JS, Dahl S, Chorkendorff I, Nørskov JK (2014) Discovery of a Ni-Ga catalyst for carbon dioxide reduction to methanol. Nat Chem 6:320–324
7. Li C, Melaet G, Ralston WT, An K, Brooks C, Ye Y, Liu Y, Zhu J, Guo J, Alayoglu S, Somorjai GA (2015) High-performance hybrid oxide catalyst of manganese and cobalt for low-pressure methanol synthesis. Nat Commun 6:6538–6542
8. Zohour B, Yilgor I, Gulgun MA, Birer O, Unal U, Leidholm C, Senkan S (2016) Discovery of superior Cu-GaOx-HoOy catalysts for the reduction of carbon dioxide to methanol at atmospheric pressure. ChemCatChem 8:1464–1469
9. Arena F, Barbera K, Italiano G, Bonura G, Spadaro L, Frusteri F (2007) Synthesis, characterization and activity pattern of Cu–ZnO/ZrO_2 catalysts in the hydrogenation of carbon dioxide to methanol. J Catal 249:185–194
10. Guo XM, Mao DS, Lu GZ, Wang S, Wu GS (2010) Glycine–nitrate combustion synthesis of CuO–ZnO–ZrO_2 catalysts for methanol synthesis from CO_2 hydrogenation. J Catal 271:178–185
11. Bonura G, Cordaro M, Cannilla C, Arena F, Frusteri F (2014) The changing nature of the active site of Cu–Zn–Zr catalysts for the CO_2 hydrogenation reaction to methanol. Appl Catal B 152–153:152–161
12. Li L, Mao DS, Yu J, Guo XM (2015) Highly selective hydrogenation of CO_2 to methanol over CuO–ZnO–ZrO_2 catalysts prepared by a surfactant–assisted co–precipitation method. J Power Sour 279:394–404
13. Witoon T, Kachaban N, Donphai W, Kidkhunthod P, Faungnawakij K, Chareonpanich M, Limtrakul (2016) Tuning of catalytic CO_2 hydrogenation by changing composition of CuO–ZnO–ZrO_2 catalysts. Energy Convers Manag 118:21–31
14. Xiao J, Mao DS, Guo XM, Yu J (2015) Methanol synthesis from CO_2 hydrogenation over CuO–ZnO–TiO_2 catalysts: the influence of TiO_2 content. Energy Technol 3:32–39

15. Zhang LX, Zhang YC, Chen SY (2012) Effect of promoter SiO_2, TiO_2 or SiO_2–TiO_2 on the performance of CuO–ZnO–Al_2O_3 catalyst for methanol synthesis from CO_2 hydrogenation. Appl Catal A 415–416:118–123
16. Xiao J, Mao DS, Guo XM, Yu J (2015) Effect of TiO_2, ZrO_2, and TiO_2-ZrO_2 on the performance of CuO-ZnO catalyst for CO_2 hydrogenation to methanol. Appl Surf Sci 338:146–153
17. Saito M, Fujitani T, Takeuchi M, Watanabe T (1996) Development of copper/zinc oxide–based multicomponent catalysts for methanol synthesis from carbon dioxide and hydrogen. Appl Catal A 138:311–318
18. Nomura N, Tagawa T, Goto S (1998) Effect of acid–base properties on copper catalysts for hydrogenation of carbon dioxide. React Kinet Catal Lett 63:21–25
19. Guo XM, Mao DS, Wang S, Wu GS, Lu GZ (2009) Combustion synthesis of CuO–ZnO–ZrO_2 catalysts for the hydrogenation of carbon dioxide to methanol. Catal Commum 10:1661–1664
20. Guo XM, Mao DS, Lu GZ, Wang S, Wu GS (2011) CO_2 hydrogenation to methanol over Cu/ZnO/ZrO_2 catalysts prepared via a route of solid–state reaction. Catal Commun 12:1095–1098
21. Angelo L, Kobl K, Tejada LMM, Zimmermann Y, Parkhomenko K, Roger A (2015) Study of CuZnMOx oxides (M=Al, Zr,Ce, CeZr) for the catalytic hydrogenation of CO_2 into methanol. C R Chimie 18:250–260.
22. Martin O, Mondelli C, Curulla–Ferre D, Drouilly C, Hauert R, Pérez–Ramírez J (2015) Zinc–rich copper catalysts promoted by gold for methanol synthesis. ACS Catal 5:5607–5616
23. Raudaskoski R, Niemelä MV, Keiski RL (2007) The effect of ageing time on co-precipitated Cu/ZnO/ZrO_2 catalysts used in methanol synthesis from CO_2 and H_2. Top Catal 45:57–60
24. Frei E, Schaadt A, Ludwig T, Hillebrecht H, Krossing I (2014) The influence of the precipitation/ageing temperature on a Cu/ZnO/ZrO_2 catalyst for methanol synthesis from H_2 and CO_2. ChemCatChem 6:1721–1730
25. Ro I, Liu Y, Ball MR, Jackson DHK, Chada JP, Sener C, Kuech TF, Madon RJ, Huber GW, Dumesic JA (2016) Role of the Cu-ZrO_2 interfacial sites for conversion of ethanol to ethyl acetate and synthesis of methanol from CO_2 and H_2. ACS Catal 6:7040–7050
26. Senanayake SD, Ramírez PJ, Waluyo I, Kundu S, Mudiyanselage K, Liu Z, Liu Z, Axnanda S, Stacchiola DJ, Evans J, Rodriguez JA (2016) Hydrogenation of CO_2 to methanol on CeOx/Cu(111) and ZnO/Cu(111) catalysts: Role of the metal–oxide interface and importance of Ce^{3+} sites. J Phys Chem C 120:1778–1784
27. López T, Alvarez M, Gómez R, Aguilar DH, Quintana P (2005) ZrO_2 and Cu/ZrO_2 sol–gel materials: spectroscopic characterization. J Sol–Gel Sci Technol 33:93–97
28. Turco M, Esposito S, Bagnasco G, Cammarano C, Pernice P, Aronne A (2010) Highly dispersed sol–gel synthesized Cu–ZrO_2 materials as catalysts for oxidative steam reforming of methanol. Appl Catal A 372:48–57
29. Huang C, Mao DS, Guo XM, Yu J (2017) Microwave-assisted hydrothermal synthesis of CuO-ZnO-ZrO_2 as catalyst for direct synthesis of methanol by carbon dioxide hydrogenation. Energy Technol 5:2100–2107
30. Fan WJ, Wu SF (2016) A graphene-supported copper-based catalyst for the hydrogenation of carbon dioxide to form methanol. J CO_2 Util 16:150–156
31. Vishwanathan V, Roh HS, Kim JW, Jun KW (2004) Surface properties and catalytic activity of TiO_2-ZrO_2 mixed oxides in dehydration of methanol to dimethyl ether. Catal Lett 96:23–28
32. Wang S, Mao DS, Guo XM, Lu GZ (2009) Dimethyl ether synthesis via CO_2 hydrogenation over CuO–TiO_2–ZrO_2/HZSM–5 bifunctional catalysts. Catal Commun 10:1367–1370
33. Ahmad R, Hellinger M, Buchholz M, Sezen H, Gharnati L, Wöll C, Sauer J, Döring M, Grunwaldt JD, Arnold U (2014) Flame-made Cu/ZnO/Al_2O_3 catalyst for dimethyl ether production. Catal Commun 43:52–56
34. Zhang MH, Liu ZM, Lin GD, Zhang HB (2013) Pd/CNT–promoted Cu–ZrO_2/HZSM–5 hybrid catalysts for direct synthesis of DME from CO_2/H_2. Appl Catal A 451:28–35
35. Słoczyński J, Grabowski R, Kozłowska A, Olszewski P, Stoch J, Skrzypek J, Lachowska M (2004) Catalytic activity of the M/($3ZnO{\cdot}ZrO_2$) system (M=Cu, Ag, Au) in the hydrogenation of CO_2 to methanol. Appl Catal A 278:11–23
36. Schumann J, Lunkenbein T, Tarasov A, Thomas N, Schlőgl R, Behrens M (2014) Synthesis and characterisation of a highly active Cu/ZnO:Al catalyst. ChemCatChem 6:2889–2897
37. Kilo M, Weigel J, Wokaun A, Koeppel RA, Stoeckli A, Baiker A (1997) Effect of the addition of chromium– and manganese oxides on structural and catalytic properties of copper/zirconia catalysts for the synthesis of methanol from carbon dioxide. J Mol Catal A 126:169–184
38. Gao P, Li F, Zhao N, Xiao F, Wei W, Zhong L, Sun Y (2013) Influence of modifier (Mn, La, Ce, Zr and Y) on the performance of Cu/Zn/Al catalysts via hydrotalcite–like precursors for CO_2 hydrogenation to methanol. Appl Catal A 468:442–452
39. Jun KW, Shen WJ, Rao KSR, Lee KW (1998) Residual sodium effect on the catalytic activity of Cu/ZnO/Al_2O_3 in methanol synthesis from CO_2 hydrogenation. Appl Catal A 174:231–238
40. Arena F, Italiano G, Barbera K, Bonura G, Spadaro L, Frusteri F (2009) Basic evidences for methanol-synthesis catalyst design. Catal Today 143:80–85
41. Natesakhawat S, Lekse JW, Baltrus JP, Ohodnicki PR, Howard Jr BH, Deng XY, Matranga C (2012) Active sites and structure–activity relationships of copper–based catalysts for carbon dioxide hydrogenation to methanol. ACS Catal 2:1667–1676
42. Karelovic A, Ruiz P (2015) The role of copper particle size in low pressure methanol synthesis via CO_2 hydrogenation over Cu/ZnO catalysts. Catal Sci Technol 5:869–881
43. Bonura G, Arena F, Mezzatesta G, Cannilla C, Spadaro L, Frusteri F (2011) Role of the ceria promoter and carrier on the functionality of Cu-based catalysts in the CO_2-to-methanol hydrogenation reaction. Catal Today 171:251–256
44. Arena F, Mezzatesta G, Zafaana G, Trunfio G, Frusteri F, Spadaro L (2013) How oxide carriers control the catalytic functionality of Cu-ZnO system in the hydrogenation of CO_2 to methanol. Catal Today 210:39–46
45. Gao P, Li F, Zhang HJ, Zhao N, Xiao F, Wei W, Zhong LS, Sun YH (2014) Fluorine-modified Cu/Zn/Al/Zr catalysts via hydrotalcite-like precursors for CO_2 hydrogenation to methanol. Catal Commun 50:78–82
46. An B, Zhang J, Cheng K, Ji P, Wang C, Lin W (2017) Confinement of ultrasmall Cu/ZnOx nanoparticles in metal–organic frameworks for selective methanol synthesis from catalytic hydrogenation of CO_2. J Am Chem Soc 139:3834–3840
47. Zhan H, Li F, Gao P, Zhao N, Xiao F, Wei W, Sun Y (2014) Influence of element doping on La–Mn–Cu–O based perovskite precursors for methanol synthesis from CO_2/H_2. RSC Adv 4:48888–48896
48. Din IU, Shaharun MS, Naeem A, Tasleem S, Johan MR (2018) Carbon nanofibers based copper/zirconia catalysts for carbon dioxide hydrogenation to methanol: Effect of copper concentration. Chem Eng J 334:619–629
49. Chalorngtham J, Witoon T, Dumrongbunditkul P, Chareonpanich M, Limtrakul J (2016) CO_2 hydrogenation to methanol over Cu/ZrO_2 catalysts: effects of zirconia phases. Chem Eng J 293:327–336
50. Pasupulety N, Driss H, Alhamed YA, Alzahrani AA, Daous MA, Petrov L (2015) Studies on Au/Cu–Zn–Al catalyst for methanol synthesis from CO_2. Appl Catal A 504:308–318